Bull. Mater. Sci., Vol. 39, No. 5, September 2016, pp. 1171–1176. © Indian Academy of Sciences.
DOI 10.1007/s12034-016-1270-3

# New $NaSrPO_4$:$Sm^{3+}$ phosphor as orange-red emitting material

**KUN-HSIEN CHEN[1], MIN-HANG WENG[2], RU-YUAN YANG[2,*] and CHENG-TANG PAN[1]**

[1]Department of Mechanical and Electro-Mechanical Engineering, National Sun Yat-Sen University, Kaohsiung County 804, Taiwan

[2]Graduate Institute of Materials Engineering, National Pingtung University of Science and Technology, Pingtung County 912, Taiwan

MS received 16 September 2015; accepted 9 March 2016

**Abstract.** **$Sm^{3+}$-activated $NaSrPO_4$ phosphors could be efficiently excited at 403 nm, and exhibited a bright red emission mainly including four wavelength peaks of 565, 600, 646 and 710 nm. The highest emission intensity was found for $NaSr_{1-x}PO_4$:$xSm^{3+}$ with a composition of $x = 0.007$. Concentration quenching was observed as the composition of $x$ exceeds 0.007. The decay time values of $NaSr_{1-x}PO_4$:$xSm^{3+}$ phosphors range from around 2.55 to 3.49 ms. $NaSr_{1-x}PO_4$:$xSm^{3+}$ phosphor shows a higher thermally stable luminescence and its thermal quenching temperature $T_{50}$ was found to be 350°C, which is higher than that of commercial YAG:$Ce^{3+}$ phosphor and ZnS:(Al, Ag) phosphor. Because $NaSr_{1-x}PO_4$:$xSm^{3+}$ phosphor features a high colour-rendering index and chemical stability, it is potentially useful as a new scintillation material for white light-emitting diodes.**

**Keywords.** **Phosphors; temperature; conventional solid-state sintering; luminescence.**

## 1. Introduction

White light-emitting diodes (W-LED) represent the fourth generation of solid-state lights, which shows promise in a wide range of applications due to low power consumption, long lifetime, low environmental and health impact and low maintenance costs [1,2]. At present, commercial white LEDs use blue LED chips (GaN or InGaN) with a yellow phosphor (YAG:$Ce^{3+}$). However, this approach suffers from some disadvantages, such as low thermal stability, poor colour performance and a narrow visible range [3]. To overcome these problems, attempts have been made to produce white light using tri-colour (RGB) phosphors excited by near-ultraviolet (NUV) light [4,5].

Several studies have reported on phosphors which emit blue or green light under UV light irradiation, such as $KSrPO_4$:$Eu^{2+}$ [2,6], $KSrPO_4$:$Tb^{3+}$ [6,7], $LiSrPO_4$:$Eu^{2+}$ [8], $NaCaPO_4$:$Eu^{2+}$ [9], $KBaPO_4$:$Eu^{2+}$ [10] and $KMgPO_4$:$Eu^{2+}$ [11] phosphors. However, red-emitting phosphors excited by NUV spectral region are lacking, and a novel red phosphor with the desired wavelength is needed.

Recently, UV-excited phosphate phosphors such as $ABPO_4$ (A = alkaline metals ($Li^+$, $Na^+$, $K^+$, $Rb^+$, $Cs^+$), B = alkaline earth metals ($Mg^{2+}$, $Ca^{2+}$, $Sr^{2+}$, $Ba^{2+}$)) have emerged as an important family of luminescent materials. The rigid tetrahedral three-dimensional matrix of phosphate is thought to be ideal for charge stabilization, thus resulting in excellent thermal stability [2].

Based on this improved thermal stability, $Eu^{3+}$, $Tb^{3+}$ and $Sm^{3+}$-activated $ABPO_4$ phosphors have been used in W-LEDs, such as $KSrPO_4$:Eu [2,6], $KSrPO_4$:Tb [6,7], $KSrPO_4$:Sm [6], $KBaPO_4$:Eu [12,13], $KBaPO_4$:Tb [12], $KBaPO_4$:Sm [12], $NaCaPO_4$:Eu [14], $NaBaPO_4$:Ce,Tb [15], $NaSrPO_4$:Eu [16–18], $NaSrPO_4$:Eu/Tb [19] and $NaSrPO_4$:Eu/Mn [20]. As a host material, $NaSrPO_4$ features a standard monoclinic crystal structure with lattice parameters with lengths $a = 2.041$ nm, $b = 0.543$ nm, $c = 1.725$ nm and angle $\beta = 101.76°$ [17,18]. Many recent studies have reported the use of Eu-doped phosphate phosphors [16–19] to produce blue emissions. Moreover, $NaSrPO_4$ phosphors co-doped with Eu/Tb ions were synthesized by a conventional solid-state reaction for blue/green emissions [19]. Red light emissions can be simply generated through NUV light excitation by doping $Sm^{3+}$ rare earth ions into a suitable host material, such as $KBaBP_2O_8$:$Sm^{3+}$ [21]. However, no studies are reported on the effect of $Sm^{3+}$ concentration on the microstructure and photoluminescence of $NaSrPO_4$ phosphors prepared by solid-state reaction sintering.

In this study, we synthesized $NaSrPO_4$ doped with various concentrations of $Sm^{3+}$ via solid-state reaction sintering. The microstructure and luminescent characteristics of the $NaSrPO_4$:$Sm^{3+}$ phosphors were investigated using X-ray diffraction (XRD), scanning electron microscopy (SEM) and photoluminescence (PL) measurements to determine the optimum concentrations of $Sm^{3+}$ ions. The impact of temperature on the photoluminescence and chromaticity of $NaSrPO_4$:$Sm^{3+}$ are also investigated. The enhancement of the thermal stability of $NaSrPO_4$:$Sm^{3+}$ for applications in W-LEDs is also discussed.

*Author for correspondence (ryyang@mail.npust.edu.tw)

## 2. Experimental

### 2.1 *Sample preparation*

In this study, $NaSr_{1-x}PO_4{:}xSm^{3+}$ ($x = 0.001$, 0.003, 0.007, 0.01, 0.02, 0.03 and 0.04) was prepared by conventional solid-state sintering. $Na_2CO_3$, $SrCO_3$, $(NH_4)_2HPO_4$ and $Sm_2O_3$ powders all with a purity of 99.9% were weighed in proper stoichiometric ratios, mixed in a ball mill for 3 h with zirconia balls and ethanol. After drying, the mixed powders were placed in a corundum crucible and sintered at 1200°C for 3 h under an air atmosphere to yield the proposed phosphors.

### 2.2 *Characterization*

The crystalline phases of the phosphors were identified using XRD (Bruker D8 Advance) analysis with CuK$\alpha$ radiation of $\lambda = 1.54$ Å, a Ni filter and a secondary graphite monochromator. A scan range of $2\theta = 10 \sim 70°$ with a step of 0.03° and 0.4 s as a per-step count time was used. Phosphor morphology was examined by SEM (HORIBA EX-200). The excitation, emission spectra and fluorescence decay time were obtained using PL measurement (JASCO FP-6000) using a 150 W xenon lamp as the light source. The specimens were measured within the same sample holder to ensure all samples had consistent amounts of phosphor material. Temperature-dependent luminescence spectra in the range of 25–450°C were detected using a FluoroLog-3 pectrofluorometer (PL, HORIBA JOBIN YVON Fluorolog-3) combined with the heating apparatus.

## 3. Results and discussion

Figure 1 shows XRD patterns of $NaSr_{1-x}PO_4{:}xSm^{3+}$ phosphors with various concentrations of $Sm^{3+}$ ions. The patterns all agreed well with JCPDS card no. 33-1282 for $NaSrPO_4$ pure phase. The XRD results show no diffraction peak shift. It can be concluded that $Sm^{3+}$ doping has no significant impact on the host structure of $NaSrPO_4$ due to the similar radius size between $Sm^{3+}$ (1.27 Å) and $Sr^{2+}$ (1.29 Å). Thus, $Sm^{3+}$ ions can partly introduced into $Sr^{2+}$ sites to keep charge balance, which supports the results reported by Cao *et al* [22]. The report indicates that the alkali metal ions are chosen as charge compensators for phosphors due to their easy entry into lattice, the small ionic radius and convenient for charge compensation.

Figure 2 shows an SEM image of $NaSr_{1-x}PO_4{:}xSm^{3+}$ phosphors with (a) $x = 0.001$, (b) $x = 0.003$, (c) $x = 0.007$, (d) $x = 0.01$, (e) $x = 0.02$, (f) $x = 0.03$ and (g) $x = 0.04$. The grain sizes of $NaSr_{1-x}PO_4{:}xSm^{3+}$ phosphors with various concentrations of $Sm^{3+}$ ions were 5–10 μm and highly aggregated. When the concentration of $Sm^{3+}$ ions is $x = 0.007$, a larger particle size was obtained. However, although all the SEM images of $NaSr_{1-x}PO_4{:}xSm^{3+}$ ($x = 0.001$, 0.003, 0.007, 0.01, 0.02, 0.03 and 0.04) phosphors reveal non-uniform and irregular structures, they still have smooth surfaces. As phosphors had crystalline powder in micrometre dimension and spherical shape, better luminescence intensities would be obtained [9].

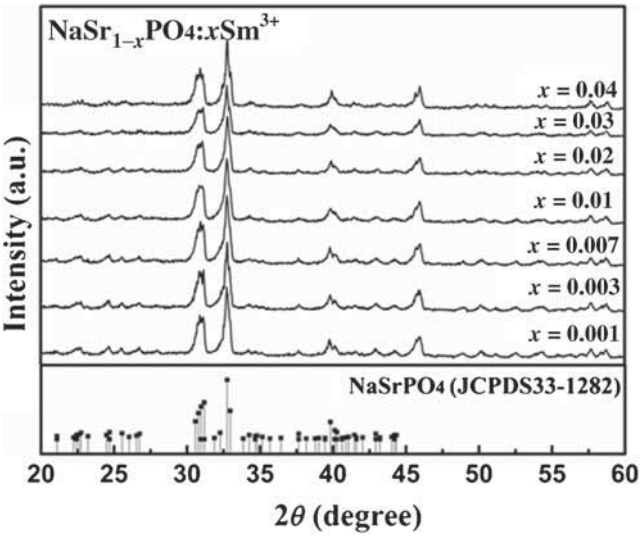


**Figure 1.** X-ray diffraction patterns of $NaSr_{1-x}PO_4{:}xSm^{3+}$ phosphors with various concentrations of $Sm^{3+}$ ions.

Figure 3 shows the excitation spectra monitored at 600 nm and emission spectrum excited at 403 nm of $NaSr_{1-x}PO_4{:}xSm^{3+}$ phosphors with various concentrations of $Sm^{3+}$ ions ($x = 0.001$, 0.003, 0.007, 0.01 and 0.04). Figure 3a show the excitation spectra of $Sm^{3+}$-doped $NaSr_{1-x}PO_4$ monitored at 600 nm consisting of several bands centred at 345, 375, 403 and 475 nm, which are the typical f–f transitions of $Sm^{3+}$ ions [6]. The strongest peak at 403 nm is attributed to the $^6H_{5/2} \rightarrow {}^4G_{7/2}$ transition of $Sm^{3+}$. PL spectra results indicate that $NaSrPO_4{:}Sm^{3+}$ phosphor is a promising red emission phosphor, and well matches the light provided by commercial NUV-LED chips. No obvious charge was found in the excitation spectrum. Typical Sm-activated phosphors exhibit charge-transfer absorption of $Sm^{3+}$–$O^{2-}$ interaction or host absorption band in the UV region. However, only direct excitation of $Sm^{3+}$ ions could be observed in this study, the interaction between $Sm^{3+}$ and the host lattice is very weak, so no energy transfer occurs between $Sm^{3+}$ and host [23].

Figure 3b shows the emission spectra of $NaSr_{1-x}PO_4{:}xSm^{3+}$ phosphors with various concentrations of $Sm^{3+}$ ions ($x = 0.001$, 0.003, 0.007, 0.01 and 0.04). At an excitation light wavelength of 403 nm, the wavelength of the emission spectrum is between 550 and 670 nm (i.e., 565, 600 and 646 nm) and another small peak at 710 nm corresponds to the $^4G_{5/2} \rightarrow {}^6H_{5/2}$, $^4G_{5/2} \rightarrow {}^6H_{7/2}$, $^4G_{5/2} \rightarrow {}^6H_{9/2}$ and $^4G_{5/2} \rightarrow {}^6H_{11/2}$ transitions of $Sm^{3+}$ ions [12]. The strongest peak at 600 nm ($^4G_{5/2} \rightarrow {}^6H_{7/2}$) is a symmetry-sensitive transition, indicating that $Sm^{3+}$ ions occupy symmetry sites of the $NaSrPO_4$ host lattice simultaneously. The luminescent intensity is also found toincrease with the increment of $Sm^{3+}$ ion doping concentration, and reaches a maximum

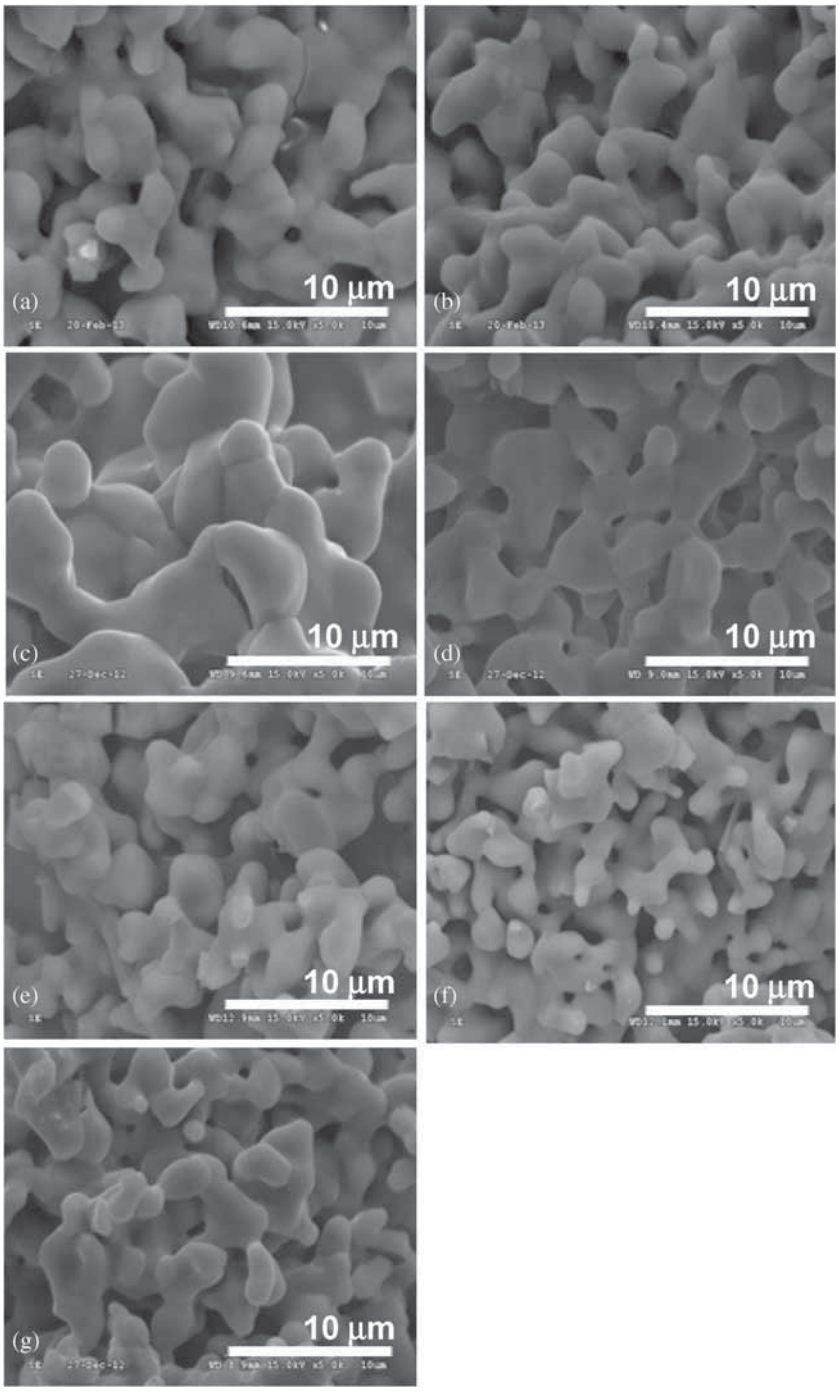


**Figure 2.** SEM images of $NaSr_{1-x}PO_4{:}xSm^{3+}$ phosphors with (**a**) $x = 0.001$, (**b**) $x = 0.003$, (**c**) $x = 0.007$, (**d**) $x = 0.01$, (**e**) $x = 0.02$, (**f**) $x = 0.03$ and (**g**) $x = 0.04$.

value at a concentration of $x = 0.007$ and then decreases as the $Sm^{3+}$ concentration $x$ exceeds 0.007, indicating that concentration quenching occurs. Thus, $x = 0.007$ is defined as the critical quenching concentration. According to Van Uitert [21], concentration quenching is mainly due to the non-radiative energy transfer among different $Sm^{3+}$ ions, which often occurs as a result of exchange interaction, radiation reabsorption, or multipole–multipole interaction. The critical distance ($R_C$) for energy transfer between host lattice and $Sm^{3+}$ ions was calculated using the concentration quenching method and the critical distance was estimated as follows [8]:

$$R_C \approx 2\left(\frac{3V}{4\pi X_C N}\right)^{1/3}, \tag{1}$$

where $V$ is the volume of the unit cell, $X_C$ the critical quenching of Sm concentration obtained from inset in figure 3b and

$N$ the number of available sites for the dopant in the unit cell. By taking $N = 16$, $V = 1.87121$ nm$^3$ and $X_C = 0.007$ for the $NaSrPO_4$ host into equation (1), the critical distance ($R_C$) was calculated to be about 3.17 nm.

On the basis of Dexter's theory [22], if the energy transfer takes place between the same kind of activators, the change in the emission intensity can determine the strength of the multipolar interaction as the multipolar interaction can take place at the emitting level. The emission intensity ($I$) per activator ion follows the following equation [8]

$$I/x = K[I + \beta(x)^{Q/3}]^{-1}, \quad (2)$$

where $x$ is the activator concentration, $I/x$ is the emission intensity ($I$) per activator concentration ($x$); $Q = 6$, 8 or 10 for dipole–dipole (d–d), dipole–quadrupole (d–q) and quadrupole–quadrupole (q–q) interactions; and $K$ and $\beta$ are constants for the same excitation condition for a given host crystal. Figure 4 shows the curve of $\log(I/x\mathrm{Sm}^{3+})$ *vs.* $\log(x\mathrm{Sm}^{3+})$ in $NaSr_{1-x}PO_4{:}x\mathrm{Sm}^{3+}$ phosphor. To obtain a $Q$ value for the emission centre the dependence of $\log(I/x\mathrm{Sm}^{3+})$ on $\log(x\mathrm{Sm}^{3+})$ is plotted in figure 4. The dependence is linear and the slope is 1.49. According to equation (2), the value of $Q$ can be calculated as 4.47, which is approximately 6. This indicates that the dipole–dipole interaction is the major mechanism for the concentration quenching of the central $Sm^{3+}$ emission in $NaSrPO_4$.

To further illustrate the colour performance of the prepared phosphors, the measured PL spectra were calculated to transform into the value of chromatic coordinates. Figure 5 shows the CIE chromaticity diagram calculated from figure 3. All the chromaticity ($x$, $y$) coordinates of the prepared $NaSr_{1-x}PO_4{:}x\mathrm{Sm}^{3+}$ phosphors with $x = 0.001$, 0.003, 0.007, 0.01, 0.02, 0.03 and 0.04 are located in the red region (0.60, 0.39). This result indicates the excellent stability of $NaSrPO_4$:Sm phosphor which will not vary with different concentrations of $Sm^{3+}$ ions. At the current stage, the poor colour rendering of commercial W-LEDs is caused by the lack of a red light component. Therefore, a red emission phosphor is needed for high colour rendering in W-LEDs.

Decay time measurement was also examined for the enhanced luminescence spectra of $NaSr_{1-x}PO_4{:}x\mathrm{Sm}^{3+}$ phosphor with various concentrations. Figure 6 shows the

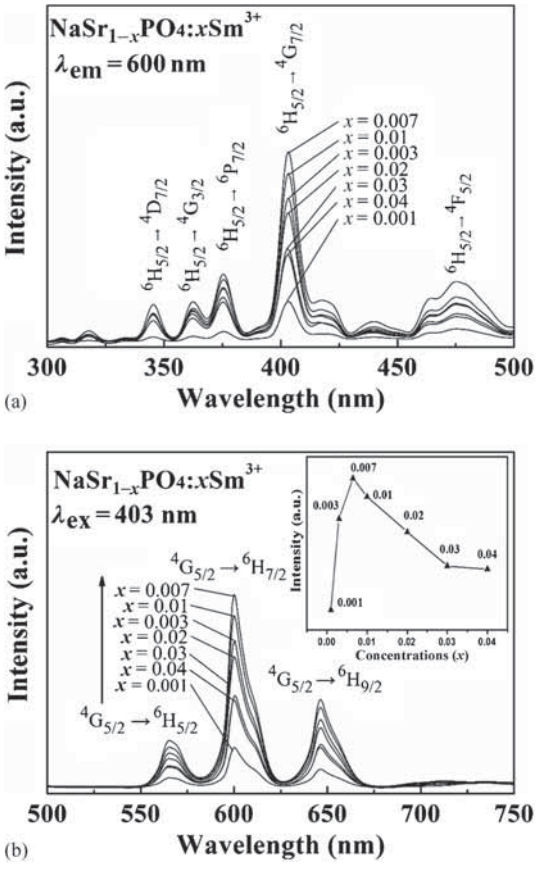


**Figure 3.** (**a**) Excitation spectra with the emission at 600 nm and (**b**) emission spectra excited at 403 nm of $NaSr_{1-x}PO_4{:}x\mathrm{Sm}^{3+}$ phosphors with various concentrations of $Sm^{3+}$ ions ($x = 0.001$, 0.003, 0.007, 0.01, 0.02, 0.03 and 0.04).

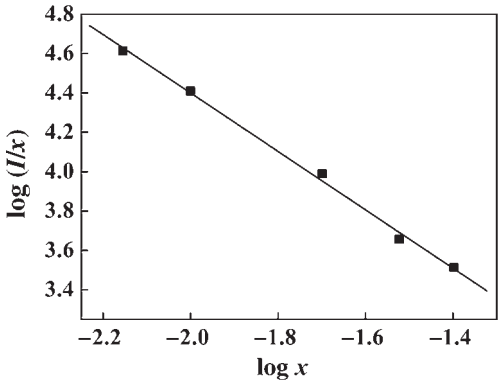


**Figure 4.** The curve of $\log(I/x\mathrm{Sm}^{3+})$ *vs.* $\log(x\mathrm{Sm}^{3+})$ in $NaSr_{1-x}PO_4{:}x\mathrm{Sm}^{3+}$ phosphor.

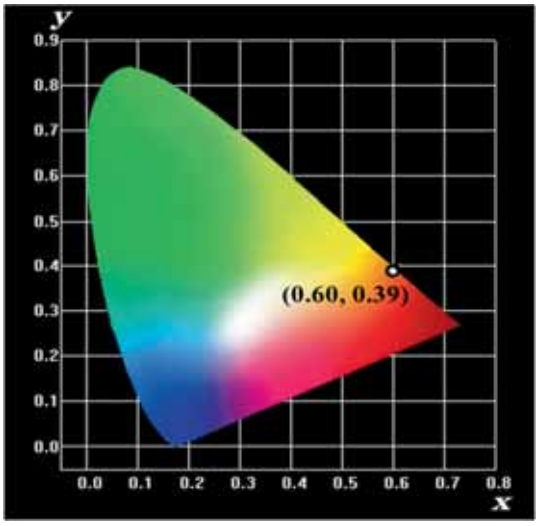


**Figure 5.** The CIE1931 chromaticity diagram of $NaSr_{1-x}PO_4{:}x\mathrm{Sm}^{3+}$ phosphors with various concentrations of $Sm^{3+}$ ions ($x = 0.001$, 0.003, 0.007, 0.01, 0.02, 0.03 and 0.04).

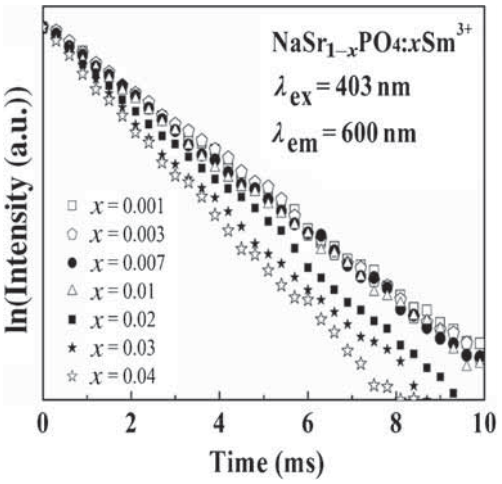


**Figure 6.** Decay time curves of $NaSr_{1-x}PO_4:xSm^{3+}$ phosphors with various concentrations of $Sm^{3+}$ ions (excited at 403 nm and monitored at 600 nm).

**Table 1.** The decay time value of $NaSr_{1-x}PO_4:xSm^{3+}$ phosphors.

| Concentration ($x$) | 0.001 | 0.003 | 0.007 | 0.01 | 0.02 | 0.03 | 0.04 |
|---|---|---|---|---|---|---|---|
| $\tau$ (ms) | 3.49 | 3.47 | 3.43 | 3.37 | 2.95 | 2.84 | 2.55 |

fluorescence decay time of 600 nm emissions for $NaSr_{1-x}PO_4:xSm^{3+}$ with $x = 0.001$, 0.003, 0.007, 0.01, 0.02, 0.03 and 0.04. The decay behaviour can be expressed as [2,7]:

$$I = I_0 \exp(-t/\tau), \tag{3}$$

where $I$ and $I_0$ are the luminescence intensities at time 0 and $t$, respectively and $\tau$ the lifetime for the exponential component. According to the parameters above, the average decay times can be calculated with equation (3) and are listed in table 1. In this study, $Sm^{3+}$ concentrations of $x = 0.001$ and 0.01 produce no obvious differences in decay times. However, when the concentration reaches $x = 0.04$, the decay time significantly decreases to 2.55 ms, a result consistent with the findings of Li *et al* [23], who observed non-exponential decay curves for higher concentrations of $Sm^{3+}$ ions ($x >$ 0.03). The non-exponential change becomes more prominent due to the inclusion of multiple relaxation processes. In addition, when the luminescent centres are located in different local environments, the associated ions will relax at different rates. The decay time of the $NaSr_{1-x}PO_4:xSm^{3+}$ phosphor gradually decreases as the concentration of $Sm^{3+}$ ions increases because of the energy transfer among $Sm^{3+}$ ions proceeds in a non-radiative manner at higher concentrations of $Sm^{3+}$ ions in the $NaSrPO_4$ host material [24].

The thermal quenching property has a significant impact on light output and colour-rendering, and thus is an important factor for applications in solid-state lighting [13]. Figure 7 shows the temperature-dependent luminescence emission intensity of the $NaSr_{0.993}PO_4$:0.007$Sm^{3+}$ excited at 403 nm,

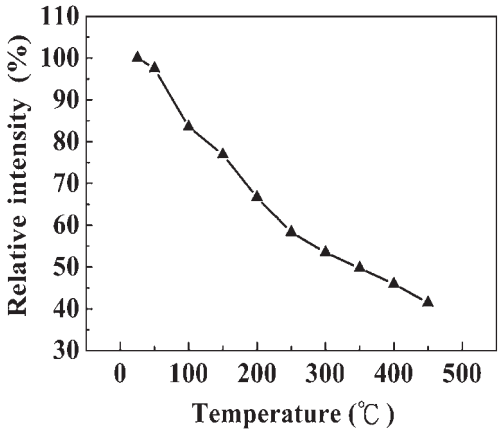


**Figure 7.** Temperature-dependent luminescent properties (excitation at 403 nm) of the $NaSr_{0.993}PO_4$:0.007$Sm^{3+}$ phosphor measured at temperatures ranging from 25 to 450°C.

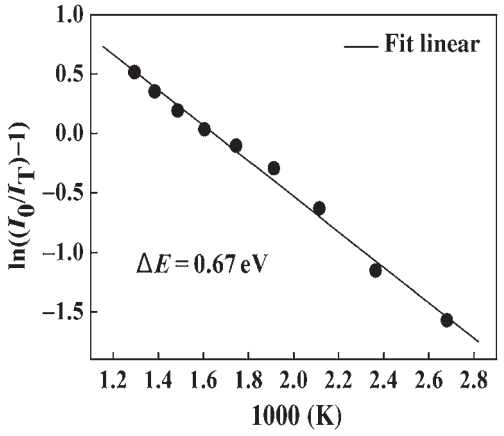


**Figure 8.** Activation energies of the thermal quenching of $NaSr_{0.993}PO_4$:0.007$Sm^{3+}$ phosphor.

monitored at 600 nm and measured at temperatures from room temperature to 450°C. In phosphors, the electrons from the lower energy excited states jump to the higher energy excited states as a result of increased temperature, and can thus generate more thermally-active phonons. The thermal quenching temperature $T_{50}$ is defined as the temperature at which the emission intensity is 50% of its original value [6]. The thermal quenching temperature $T_{50}$ of $NaSr_{0.993}PO_4$:0.007$Sm^{3+}$ phosphor was found to be 350°C, indicating that the prepared phosphate powders have a better $T_{50}$ than that of commercial YAG:$Ce^{3+}$ [12] and ZnS:(Al, Ag) phosphors [17]. The excellent thermal and chemical stabilities of $NaSr_{0.993}PO_4$:0.007$Sm^{3+}$ phosphor make it suitable for use as an RGB luminescent material in W-LEDs [6].

The thermal quenching behaviour at various temperatures could be understood by fitting the Arrhenius equation [13]:

$$I_T = \frac{I_0}{1 + c\exp(-(\Delta E/kT))}, \tag{4}$$

where $I_0$ is the initial intensity, $I_T$ the intensity at different temperatures, $\Delta E$ the activation energy of thermal quenching, $c$ a constant and $k$ the Boltzmann constant ($8.629 \times 105$ eV). According to equation (4), the calculated activation energy of the thermal quenching of the $NaSr_{0.993}PO_4{:}0.007Sm^{3+}$ phosphor was 0.67 eV as shown in figure 8. The value of the activation energy $\Delta E$ is similar to that obtained by Sun *et al* [24]. Our results follow the general rule that the emission peak with the lower Stokes shift has a higher activation energy and a higher quenching temperature [12].

## 4. Conclusion

$NaSr_{1-x}PO_4{:}xSm^{3+}$ f–f transition phosphors were successfully prepared by high temperature solid state sintering at 1200°C for 3 h under an air atmosphere. XRD results show pure phases of $NaSr_{1-x}PO_4{:}xSm^{3+}$ phosphors and no diffraction peak shift. The average particle sizes are estimated in the range of 5–10 μm. The phosphor produces a multi-emission band upon excitation at a light wavelength of 403 nm, which is close to near-ultraviolet excitation. Moreover, the optimum concentrations for $Sm^{3+}$ were determined to be $x = 0.07$ in $NaSr_{1-x}PO_4{:}xSm^{3+}$. It was found that the major mechanism for concentration quenching occurred as a result of dipole–dipole interaction according to Dexter's theory. In addition, the thermal quenching temperature $T_{50}$ was found to be 350°C, which is higher than that of commercial YAG:$Ce^{3+}$ phosphor and ZnS:(Al, Ag) phosphor. It is suggested that $NaSrPO_4{:}Sm^{3+}$ phosphors have potential for application in W-LEDs.

## Acknowledgements

This study was funded by the Ministry of Science and Technology, Bureau of Energy, the Ministry of Economic Affairs and the Southern Taiwan Science Park Administration (STSPA), Taiwan, The Republic of China under contracts NSC 101-2628-E-020-002-MY3, nos. 102-E0603 and 102GE06. We would also like to thank the National Nano-Device Laboratories and the Precision Instrument Center of National Pingtung University of Science and Technology, for supplying experimental equipment.

## References

[1] Sheu J K, Chang S J, Kuo C H, Su Y K, Wu L W, Lin Y C *et al* 2003 *IEEE Photonic. Tech. L.* **15** 18
[2] Su Y K, Peng Y M, Yang R Y and Chen J L 2012 *Opt. Mater.* **34** 1598
[3] Kim J S, Jeon P E, Park Y H, Choi J C, Park H L, Kim G C and Kim T W 2004 *Appl. Phys. Lett.* **85** 3696
[4] Yang R Y, Chen H Y, Hsiung C M and Chang S J 2011 *Ceram. Int.* **37** 749
[5] Lin C C, Xiao Z R, Guo G Y, Chan T S and Liu R S 2010 *J. Am. Chem. Soc.* **132** 3020
[6] Lin C C, Liu R S, Tang Y S and Hu S F 2008 *J. Electrochem. Soc.* **155** J248
[7] Weng M H, Yang R Y, Peng Y M and Chen J L 2012 *Ceram. Int.* **38** 1319
[8] Wu Z C, Shi J, Wang J, Gong M L and Su Q 2006 *J. Solid State Chem.* **179** 2356
[9] Grandhe B K, Bandi V R, Jang K, Kim S S, Shin D S, Lee Y I *et al* 2011 *J. Alloys Compd.* **509** 7937
[10] Poort S H M, Janssen W and Blasse G 1997 *J. Alloys Compd.* **260** 93
[11] Zhang S Y, Huang Y L and Seo H J 2010 *Opt. Mater.* **32** 1545
[12] Lin C C, Tang Y S, Hu S F and Liu R S 2009 *J. Lumin.* **129** 1682
[13] Zhang S Y, Nakai Y, Tsuboi T, Huang Y L and Seo H J 2011 *Inorg. Chem.* **50** 2897
[14] Peng Y M, Su Y K and Yang R Y 2013 *Mater. Res. Bull.* **48** 1946
[15] Dou X H, Zhao W R, Song E H, Deng L L, Fang X B and Min H C 2012 *J. Rare Earth* **30** 739
[16] Yim D K, Song H J, Cho I S, Kim J S and Hong K S 2011 *Mater. Lett.* **65** 1666
[17] Tung Y L and Jean J H 2009 *J. Am. Ceram. Soc.* **92** 1860
[18] Sun J Y, Zhang X Y, Zhu J C, Sun Y and Du H Y 2012 *Adv. Mater. Res.* **502** 128
[19] Sun J Y, Zhu J C, Zhang X Y, Xia Z G and Du H Y 2012 *J. Lumin.* **132** 2937
[20] Li Y, Li H R, Liu B T, Zhang J, Zhao Z Y, Yang Z G *et al* 2013 *J. Phys. Chem. Solids* **74** 175
[21] Vanuitert L G 1984 *J. Lumin.* **29** 1
[22] Dexter D L 1953 *J. Chem. Phys.* **21** 836
[23] Li Y C, Chang Y H, Lin Y F, Chang Y S and Lin Y J 2007 *J. Alloys Compd.* **439** 367
[24] Sun J Y, Zhang X Y, Xia Z G and Du H Y 2012 *J. Appl. Phys.* **111** 013101